Synergistic Experimental and Theoretical Investigation of Carbazole-Cyanopyridine-Based Hole-Transporting Materials

Rachel Chetri,[a] Vygintas Jankauskas,[b] Gediminas Kreiza,[d] Kasparas Rakstys,[c] Vytautas Getautis,[c] Rahim Ghadari,[e] Arijit Saha,[a] and Ahipa Tantri Nagaraja [a]*

[a] Centre for Nano and Material Sciences, Jain (Deemed-to-be University), Jain Global Campus, Kanakapura, Bangalore, Karnataka, India – 562112

[b] Institute of Chemical Physics, Vilnius University, Saulėtekio al. 3, 10257 Vilnius, Lithuania

[c] Department of Organic Chemistry, Kaunas University of Technology, Radvilenu pl. 19, Kaunas 50254, Lithuania

[d] Institute of Photonics and Nanotechnology, Vilnius University, Saulėtekio al. 3, 10257 Vilnius, Lithuania

[e] Computational Chemistry Laboratory, Department of Organic and Biochemistry, Faculty of Chemistry, University of Tabriz, Tabriz 5166616471, Iran

*Corresponding Author email address: tn.ahipa@jainuniversity.ac.in

Contents

1. Experimental:

General Aspects:

N-Ethylcarbazole was procured from BLD Pharmatech (India) Pvt. Ltd., ammonium acetate, and ethylcyanoacetate were procured from TCI. 1-Bromohexane, and K_2CO_3 were purchased from Sigma-Aldrich (India), and 1,4-dioxane was procured from Avra Synthesis Pvt. Ltd., Telangana, India, and solvents were procured from Pure Chems. IR spectra were collected using Bruker ALPHA eco-ATR-IR on ZnSe Crystal. ^{1}H and ^{13}C NMR spectra were

obtained using 400 MHz and 100 MHz Bruker spectrometer with DMSO-d_6 as solvent and TMS as internal standard. High-resolution mass spectrometry (MS) was obtained from a Waters, USA XEVO-G2-XS-QTOF Mass spectrometer. UV-visible absorption and emission properties were measured using UV-1800 SHIMADZU UV-spectrophotometer and RF-5301 PC, SHIMADZU spectrophotometer equipped with a Xe-lamp as an excitation source, respectively.

Cyclic voltammetry (CV) data were determined in a N_2-saturated three-electrode system, where, the working, counter, and reference electrodes are glassy carbon, platinum, and Ag/Ag^+, respectively. The glassy carbon electrode was polished with 1.0μm alumina slurry and then sonicated for 10 min in distilled water. **DJ01-alkyl, PR01-alkyl,** and **PM01-alkyl** in THF (1 mg/mL) were drop casted on to the glassy carbon disk and dried to get a uniform thin film, which was later dipped into the acetonitrile solution containing 0.1 M tetrabutylammonium hexafluorophosphate ($TBAPF_6$) as the supporting electrolyte. Further, the electrochemical measurements were made at a scan rate of 100 mV/s. The Ag/Ag^+ reference electrode was calibrated using a ferrocene/ ferrocenium (Fc/Fc^+) redox couples as an external standard.

Thermogravimetric analyses (TGA) and Differential scanning calorimetry (DSC) were performed on a STA 6000 Simultaneous Thermal Analyzer instrument under nitrogen gas atmosphere at a heating rate of 10 °C/min. Contact angle measurement to assess hydrophilicity was conducted using a TECH Contact angle measurement instrument (Model No: TECH CON-1200). Single crystals of **DJ01-alkyl** and **PR01-alkyl** were grown from tetrahydrofuran solvent at room temperature. Suitable single crystal was selected under microscope, mounted on a microloop (MiTeGen) using inert oil and analyzed on a XtaLab Synergy (Rigaku) diffractometer equipped with HyPix-6000HE detector and PhotonJet X-ray source (CuKα, λ = 1.54184) at 100.0 K. Data was collected and processed with CrysAlisPro software. The structures were solved by Intrinsic Phasing with the ShelXT[1] program and refined with the ShelXL[2] package using Least Squares minimization as implemented in Olex2 graphical interface.[3] The structure files were deposited with the Cambridge Crystallographic Data Centre (CCDC, deposition number (2500277 and 2455342) and can be accessed free of charge. The mixture of PbI_2 and CH_3NH_3I in 1:1 ratio was dissolved in a mixture of DMF and DMSO (7:3 (v/v) mixture; >98%, Tokyo chemical industry) at 1.0 M and stirred overnight.[4] The precursor layer was annealed on a hotplate at 100 °C for 10 min. After cooling down to room temperature, the HTMs (1mg/mL in chlorobenzene) was subsequently deposited on top of the perovskite layer by spin coating.

The xerographic time-of-flight (XTOF) technique was used to characterize charge transport in the films of **DJ01-alkyl - PM01-alkyl** materials. Samples are prepared under drop casting technique on Al coated glass plates using THF or CB (**DJ04-alkyl**) as solvent. Sample thickness was 2.2-3.3 μm. The corona charging used to create electric field in the sample. Charge carriers were generated at the layer surface by illumination with pulses of nitrogen laser (pulse duration was 1 ns, wavelength 337 nm). The layer surface potential decrease as a result of pulse illumination was about 3-10 % of initial potential. The capacitance probe deposited over the sample and connected to the wide frequency band electrometer measured the speed of the surface potential decrease d*U*/d*t*, which is equivalent to a current in widely known TOF technique. The transit time t_t was determined by the kink on the curve of the d*U*/d*t* transient in double logaritmic scale. These materials are characterized by dispersive charge transport. The drift mobility was calculated by the formula $\mu = d^2/U_0 t_t$, where d is the layer thickness and U_0 is the surface potential at the moment of illumination. The hole mobility results are shown in standard plot for organic compounds.

1.2. Synthetic Procedure:

1.2.1. Synthesis of 4-(9-ethyl-9*H*-carbazol-3-yl)-2-(hexyloxy)-6-(thiophen-2-yl)nicotinonitrile (DJ01-alkyl).

To a mixture of compound DJ01 (0.5 g, 1.26 mmol) and 1-bromohexane (212 mg, 1.5 mmol) in DMF (8 mL), 1.2 eq. of K_2CO_3 (262 mg) was added and stirred for 24 h at 80 °C. After cooling and quenching the mixture in ice-cold water, a precipitate was obtained. This precipitate was then filtered and purified using column chromatography on silica gel with ethyl acetate/hexane (v/v, 2:98) to get the yellowish white product **DJ01-alkyl** (425 mg, yield: 70.1%). mp: 135-137 ºC; ATR-IR (cm^{-1}): 2917 (C-H), 2216 (C≡N) and 1583 (C=N). ^{1}H NMR (400 MHz, DMSO-d_6), δ (ppm): 8.58 (d, J = 1.1 Hz, 1H), 8.25 (d, J = 7.7 Hz, 1H), 8.11 (dd, J = 3.7, 0.9 Hz, 1H), 7.89 – 7.76 (m, 4H), 7.69 (d, J = 8.3 Hz, 1H), 7.62 – 7.47 (m, 1H), 7.40 – 7.08 (m, 2H), 4.52 (q, J = 6.3 Hz, 4H), 1.82 (dd, J = 14.5, 6.8 Hz, 2H), 1.53 – 1.41 (m, 2H), 1.34 (dt, J = 12.3, 6.6 Hz, 7H), 0.89 (t, J = 7.0 Hz, 3H). ^{13}C NMR (100 MHz, DMSO-d_6), δ (ppm): 164.67, 157.62, 152.89, 144.43, 143.31, 142.39, 140.79, 140.56, 129.40, 128.78, 126.91, 126.62, 126.59, 121.51, 119.86, 116.40, 112.52, 109.98, 67.54, 37.65, 31.39, 29.65, 25.51, 22.51, 14.32, 14.19; HR-ESI-TOF MS: m/z = 479.3417 (calculated for $C_{30}H_{29}N_3OS$:479.2031 $[M]^+$).

1.2.2. Synthesis of 6-(4-bromophenyl)-4-(9-ethyl-9H-carbazol-3-yl)-2-(hexyloxy)nicotinonitrile (PR01-alkyl).

To a mixture of compound PR01 (0.5 g, 1.06 mmol) and 1-bromohexane (179 mg, 1.28 mmol) in DMF (8 mL), 1.2 eq. of K_2CO_3 (221 mg) was added and stirred for 24 h at 80 °C. After cooling and quenching the mixture in ice-cold water, a precipitate was obtained. This precipitate was then filtered and purified using column chromatography on silica gel with ethyl acetate/hexane (v/v, 2:98) to get the yellowish white product **PR01-alkyl** (435 mg, yield: 73.9%). mp: 135-137 ºC; ATR-IR (cm^{-1}): 2917 (C-H), 2214 (C≡N) and 1581 (C=N). ^{1}H NMR (400 MHz, DMSO-d_6), δ (ppm): 8.62 (d, J = 1.5 Hz, 1H), 8.31 – 8.15 (m, 3H), 7.93 (s, 1H), 7.88 (dd, J = 8.6, 1.8 Hz, 1H), 7.81 (d, J = 8.6 Hz, 1H), 7.77 – 7.75 (m, 1H), 7.75 – 7.73 (m, 1H), 7.69 (d, J = 8.3 Hz, 1H), 7.60 – 7.49 (m, 1H), 7.34 – 7.21 (m, 1H), 5.31 – 3.94 (m, 4H), 1.97 – 1.70 (m, 2H), 1.48 (dd, J = 14.9, 7.0 Hz, 2H), 1.43 – 1.27 (m, 7H), 0.89 (t, J = 7.1 Hz, 3H). ^{13}C NMR (100 MHz, DMSO-d_6), δ (ppm): 164.72, 157.77,156.03, 140.80, 140.54, 136.48, 132.23, 129.78, 127.27, 126.89, 126.66, 126.53, 124.73, 122.91,122.59, 121.64, 121.31, 121.16, 119.84, 116.32, 114.19,109.73, 92.85, 67.49, 31.31, 28.68, 28.35, 25.56, 22.51, 14.82, 14.32, 14.18; HR-ESI-TOF MS: m/z = 552.1652 (calculated for $C_{32}H_{30}BrN_3O$:552.1650 $[M+H]^+$).

1.2.3. Synthesis of 4-(9-ethyl-9*H*-carbazol-3-yl)-2-(hexyloxy)-6-(4-nitrophenyl)nicotinonitrile (PM01-alkyl).

To a mixture of compound PM01 (0.5 g, 1.15 mmol) and 1-bromohexane (190 mg, 1.38 mmol) in DMF (8 mL), 1.2 eq. of K_2CO_3 (238 mg) was added and stirred for 24 h at 80 °C. After cooling and quenching the mixture in ice-cold water, a precipitate was obtained. This precipitate was then filtered and purified using column chromatography on silica gel with ethyl acetate/hexane (v/v, 2:98) to get the yellowish white product **PM01-alkyl** (412 mg, yield: 69.1%). mp: 135-137 ºC; ATR-IR (cm^{-1}): 2917 (C-H), 2212 (C≡N) and 1584 (C=N). ^{1}H NMR (400 MHz, DMSO-d_6), δ (ppm): 8.60 (d, *J* = 1.5 Hz, 1H), 8.47 (d, *J* = 8.9 Hz, 2H), 8.27 (dd, *J* = 31.7, 8.3 Hz, 3H), 8.01 (s, 1H), 7.79 (ddd, *J* = 46.2, 23.1, 5.0 Hz, 3H), 7.52 (dd, *J* = 11.3, 4.0 Hz, 1H), 7.27 (t, *J* = 7.4 Hz, 1H), 4.51 (dt, *J* = 14.1, 6.7 Hz, 4H), 1.93 – 1.67 (m, 2H), 1.41 – 1.26 (m, 9H), 0.87 (dd, *J* = 13.3, 6.2 Hz, 3H. ^{13}C NMR (100 MHz, DMSO-d_6), δ (ppm): 164.7, 158.0, 154.6, 148.7, 143.2, 140.8, 140.5, 129.0, 126.7, 126.2, 124.3, 122.9, 122.5, 121.7, 119.9,115.6, 110.0, 109.8, 94.0, 67.72, 37.65, 34.65, 31.98, 31.78, 31.41, 28.67, 26.80, 25.56,

22.51, 14.32, 14.19; HR-ESI-TOF MS: m/z = 519.2399 (calculated for $C_{32}H_{30}N_4O_3$:519.2396 $[M+H]^+$).

2. Cost Calculation

Table S1: Calculated cost for the synthesis of **DJ01-alkyl**.

Chemical	**Vendor**	**Weight of reagent (g)**	**Price (Rs)**	**Amount require (g)**	**Price (Rs)**
DJ01	synthesized	1	656	0.5	328
K_2CO_3	Sigma	500	10220	0.262	5.3
Hexyl bromide	Spectrochem	250 ml	1950	0.21	1.6
DMF	Sigma	2 L	16941	0.01	84
Total cost	418.9				
Amount of DJ01-alkyl	0.44 g				
Total cost of DJ01-alkyl	952 (Rs) or 11.41 ($)				

Table S2: Calculated cost for the synthesis of **PR01-alkyl**.

Chemical	**Vendor**	**Weight of reagent (g)**	**Price (Rs)**	**Amount require (g)**	**Price (Rs)**
PR01	synthesized	1	687	0.5	343
K_2CO_3	Sigma	500	10220	0.221	4.5
Hexyl bromide	Spectrochem	250 ml	1950	0.179	1.39
DMF	Sigma	2 L	16941	0.01	84
Total cost	432				
Amount of PR01-alkyl	0.435 g				
Total cost of PR01-alkyl	993 (Rs) or 11.90 ($)				

Table S3: Calculated cost for the synthesis of **PM01-alkyl**.

Chemical	**Vendor**	**Weight of reagent (g)**	**Price (Rs)**	**Amount require (g)**	**Price (Rs)**
PM01	synthesized	1	579	0.5	289
K_2CO_3	Sigma	500	10220	0.238	4.8
Hexyl bromide	Spectrochem	250 ml	1950	0.19	1.4
DMF	Sigma	2 L	16941	0.01	84
Total cost	379				
Amount of PM01-alkyl	0.385				
Total cost of PM01-alkyl	984 (Rs) or 11.79 ($)				

Table S4: Summary of cost calcaultion of various carbazole based HTMs.

HTMs	**cost/g ($)**	**Ref.**
DJ01-alkyl	**11.41**	**This work**
PR01-alkyl	**11.90**	**This work**
PM01-alkyl	**11.79**	**This work**
3,6-Pyr	**28.30**	[5]
CZ-TA	**25.00**	[6]
YT-KTPA	**37.14**	[7]
CS-05	**42.08**	[8]
LD29	**30.20**	[9]
LD22	**33.20**	[10]
H-Ca	**22.20**	[11]
Car[2,3]	**27.00**	[12]
Spiro-OMeTAD	**400.00**	[13]

Table S5: Solubility limits of **DJ01-alkyl, PR01-alkyl** and **PM01-alkyl** in different solvents.

Solvent	**Solubility Limit (mg/ml)**					
	DJ01-alkyl	**PR01-alkyl**	**PM01-alkyl**	**DJ01[a]**	**PR01[a]**	**PM01[a]**
Dimethyl sulphoxide	70 mg/ml	70 mg/ml	70 mg/ml	5 mg/ml	5 mg/ml	5 mg/ml
N,*N*-Dimethylformamide	70 mg/ml	70 mg/ml	70 mg/ml	5 mg/ml	5 mg/ml	5 mg/ml
Ethyl acetate	68 mg/ml	68 mg/ml	68 mg/ml	Insoluble	Insoluble	Insoluble
Tetrahydrofuran	70 mg/ml	70 mg/ml	70 mg/ml	1 mg/ml	1 mg/ml	1 mg/ml

Dichloromethane	67 mg/ml	67 mg/ml	67 mg/ml	0.5 mg/ml	0.5 mg/ml	0.5 mg/ml
Chloroform	60 mg/ml	60 mg/ml	60 mg/ml	0.5 mg/ml	0.5 mg/ml	0.5 mg/ml
Chlorobenzene	68 mg/ml	68 mg/ml	68 mg/ml	1 mg/ml	1 mg/ml	1 mg/ml
Hexane	68 mg/ml	68 mg/ml	68 mg/ml	Insoluble	Insoluble	Insoluble

Here a= Previously synthesized compounds.[14]

3. Crystal Data:

Table S6: Crystallographic data of **DJ01-alkyl** and **PR01-alkyl**.

Empirical formula	$C_{30}H_{29}N_3OS$	$C_{35}H_{32.5}BrCl_{0.5}N_3O$
Formula weight	479.65	608.77
Temperature/K	296.0(9)	100.00(10)
Crystal system	monoclinic	monoclinic
Space group	$P2_1/c$	C2/c
a/Å	20.0534(5)	42.0517(6)
b/Å	11.8621(3)	7.42350(10)
c/Å	10.8047(2)	18.4826(3)
α/°	90	90
β/°	92.512(2)	96.0880(10)
γ/°	90	90
Volume/Å^3	2567.70(10)	5737.19(15)
Z	4	8
ρ_{calc}g/cm^3	1.241	1.410
μ/mm^{-1}	1.326	2.637
F(000)	1016.0	2520.0
Crystal size/mm^3	0.268 × 0.109 × 0.019	0.276 × 0.089 × 0.024
Radiation	Cu Kα (λ = 1.54184)	Cu Kα (λ = 1.54184)
2Θ range for data collection/°	4.41 to 154.332	4.226 to 154.312
Index ranges	-25 ≤ h ≤ 22, -11 ≤ k ≤ 14, -13 ≤ l ≤ 13	-52 ≤ h ≤ 49, -7 ≤ k ≤ 9, -23 ≤ l ≤ 22
Reflections collected	15967	15346
Independent reflections	5213 [R_{int} = 0.0372, R_{sigma} = 0.0442]	5672 [R_{int} = 0.0325, R_{sigma} = 0.0281]
Data/restraints/parameters	5213/0/318	5672/0/337
Goodness-of-fit on F^2	1.049	1.073
Final R indexes [I>=2σ (I)]	R_1 = 0.0501, wR_2 = 0.1439	R_1 = 0.0546, wR_2 = 0.1628
Final R indexes [all data]	R_1 = 0.0636, wR_2 = 0.1547	R_1 = 0.0559, wR_2 = 0.1636
Largest diff. peak/hole / e Å^{-3}	0.28/-0.41	2.14/-0.82

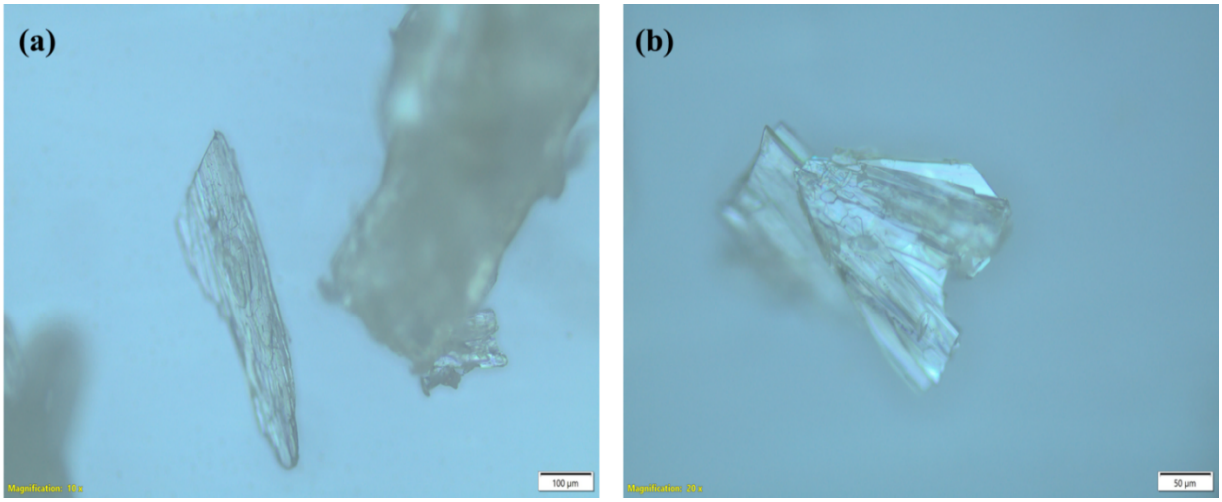

Fig. S1: Crystals of (a) **DJ01-alkyl** and (b) **PR01-alkyl** under optical microscope.

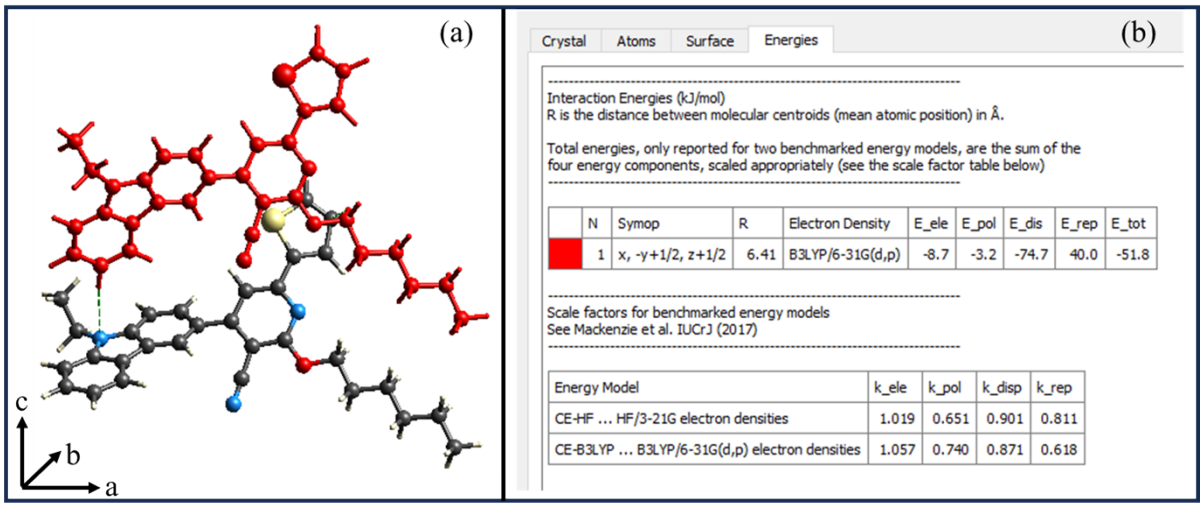

	N	Symop	R	Electron Density	E_ele	E_pol	E_dis	E_rep	E_tot
	1	x, -y+1/2, z+1/2	6.41	B3LYP/6-31G(d,p)	-8.7	-3.2	-74.7	40.0	-51.8

Energy Model	k_ele	k_pol	k_disp	k_rep
CE-HF ... HF/3-21G electron densities	1.019	0.651	0.901	0.811
CE-B3LYP ... B3LYP/6-31G(d,p) electron densities	1.057	0.740	0.871	0.618

Fig. S2. Crystal explorer-based energy frameworks, different types of interaction energies along the direction of intermolecular hydrogen-bond for the **DJ01-alkyl** crystals with a 100-energy scale factor and a zero-energy threshold.

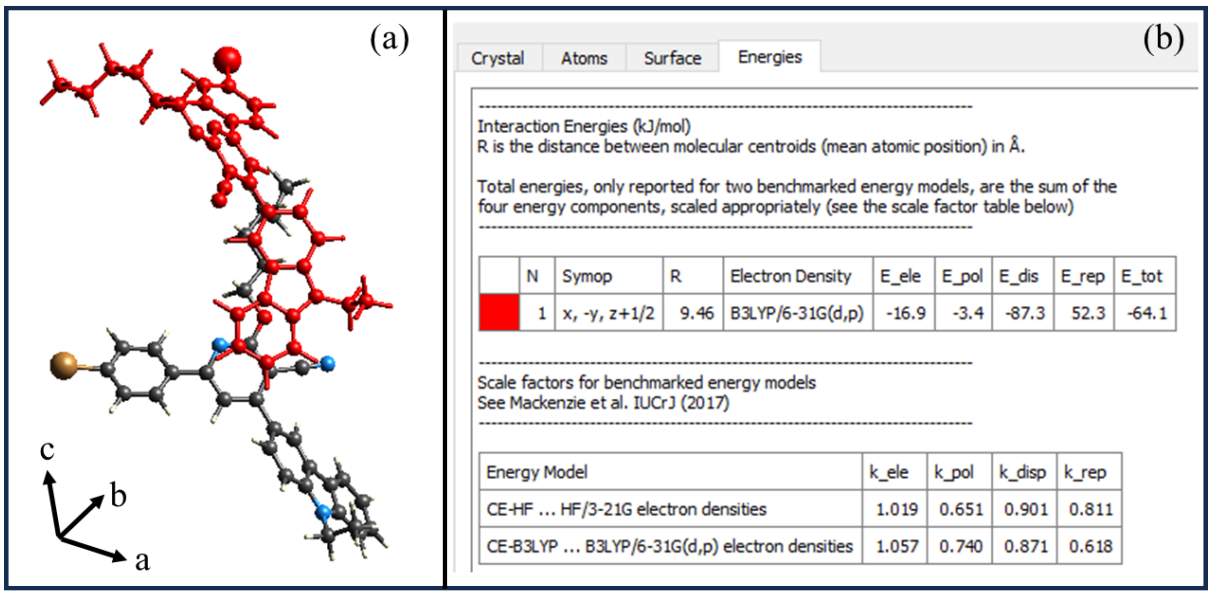

Fig. S3. Crystal explorer-based energy frameworks, different types of interaction energies along the direction of π-π interactions for the **PR01-alkyl** with a 100-energy scale factor and a zero-energy threshold.

4. ATR-IR Spectra:

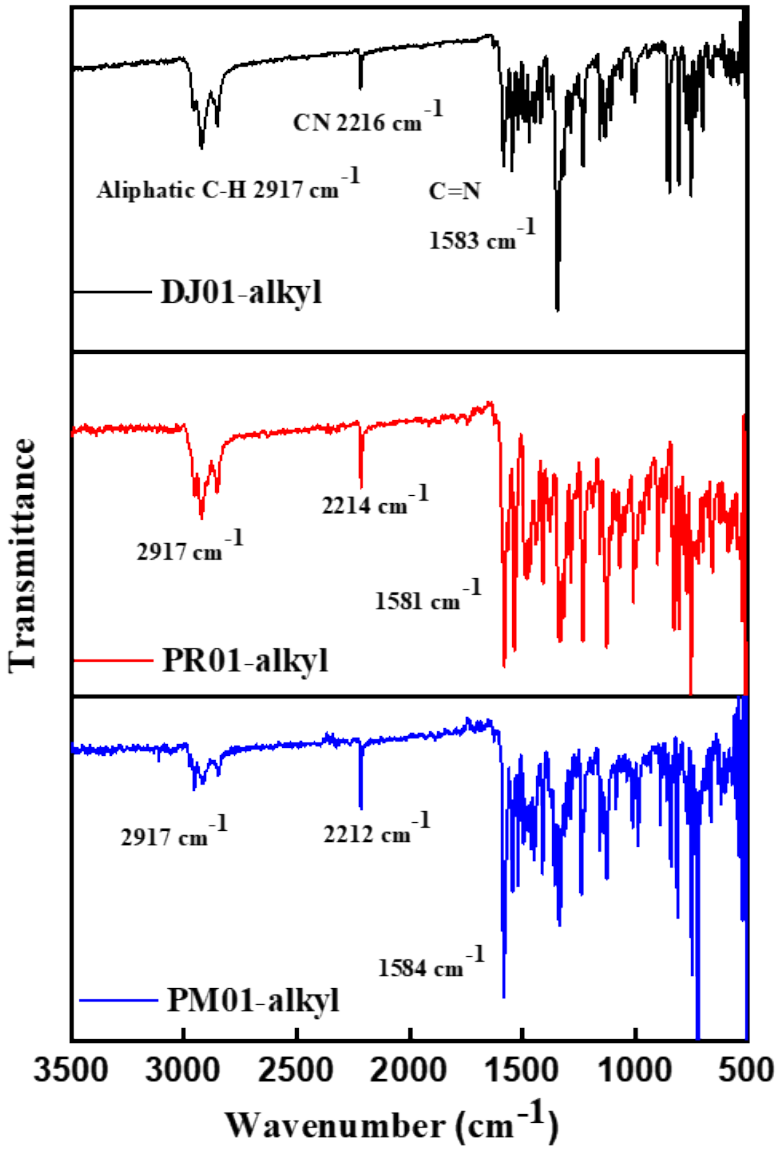

Fig. S4: ATR-IR spectra of **DJ01-alkyl, PR01-alkyl**, and **PM01-alkyl**.

5. ^{1}H NMR and ^{13}C NMR Spectra:

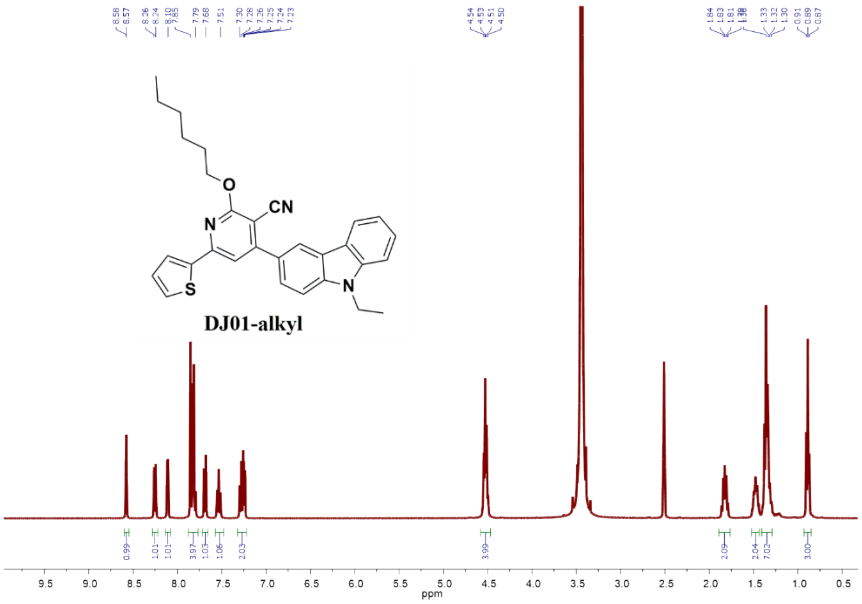

Fig. S5: ^{1}H NMR spectrum (400 MHz, DMSO-d_6) of **DJ01-alkyl**.

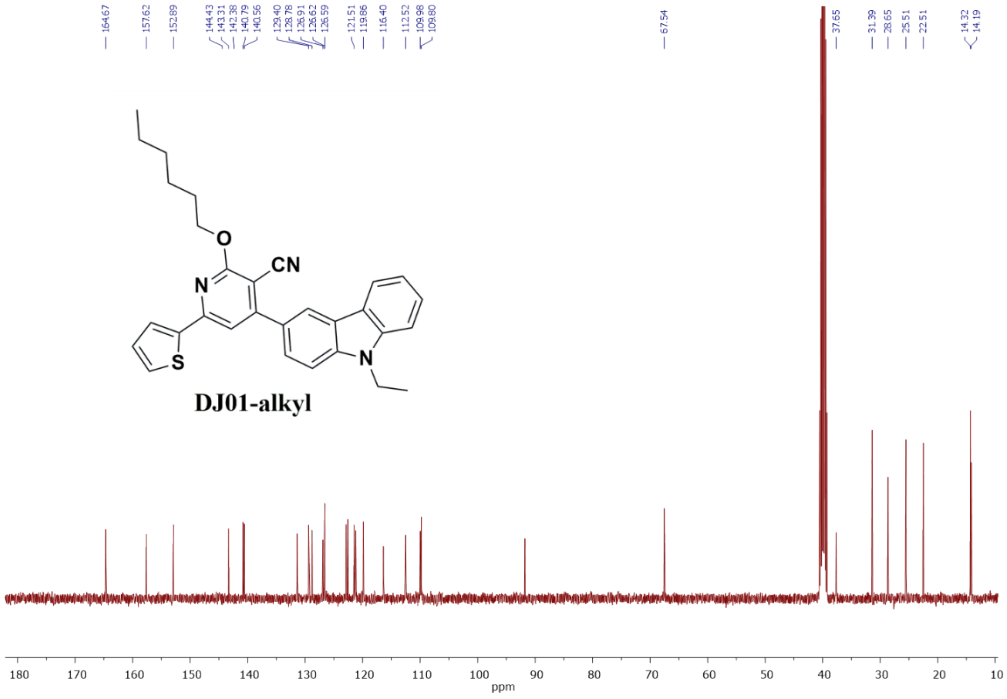

Fig. S6: ^{13}C NMR spectrum (100 MHz, DMSO-d_6) of **DJ01-alkyl**.

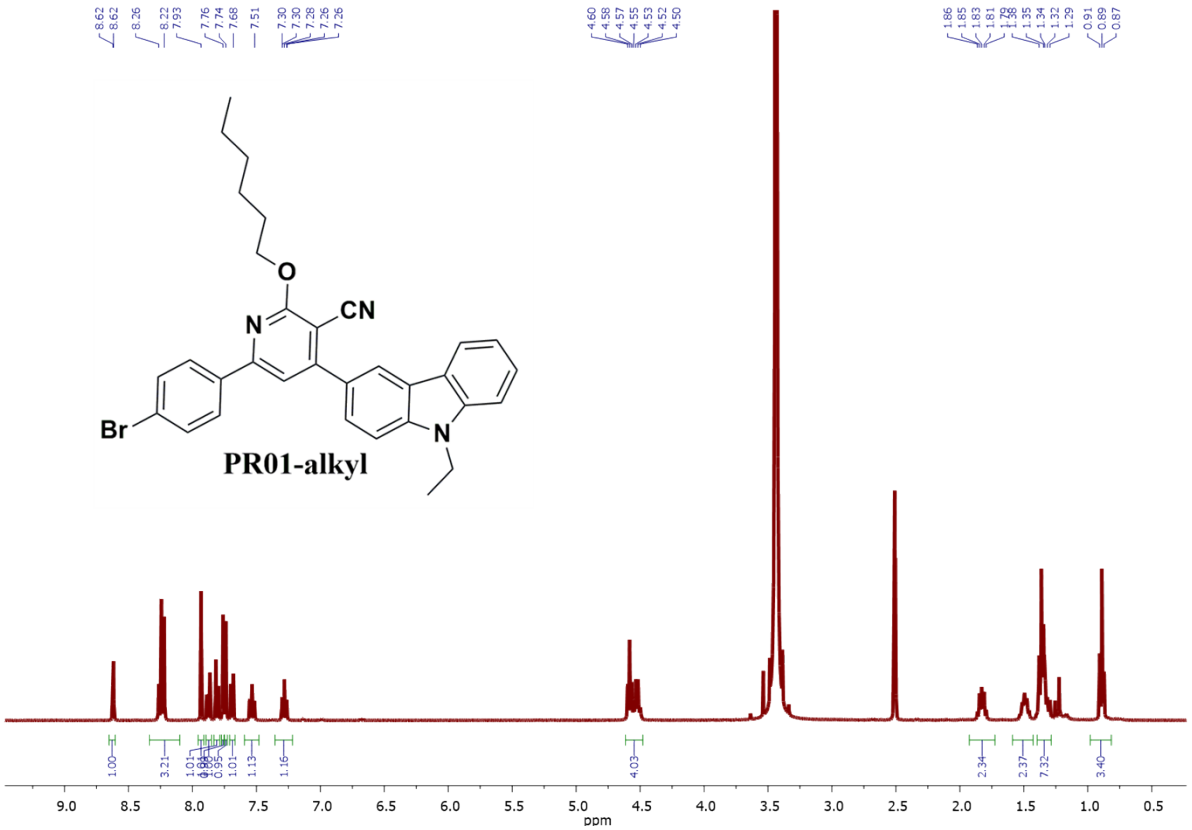

Fig. S7: ^{1}H NMR spectrum (400 MHz, DMSO-d_6) of **PR01-alkyl**.

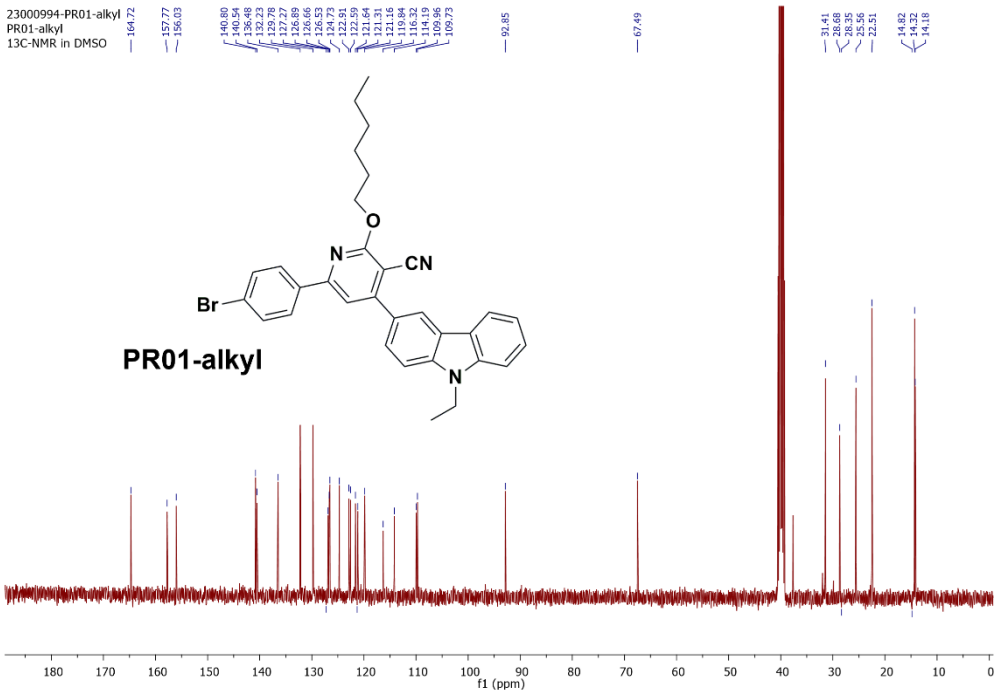

Fig. S8: ^{13}C NMR spectrum (100 MHz, DMSO-d_6) of **PR01-alkyl.**

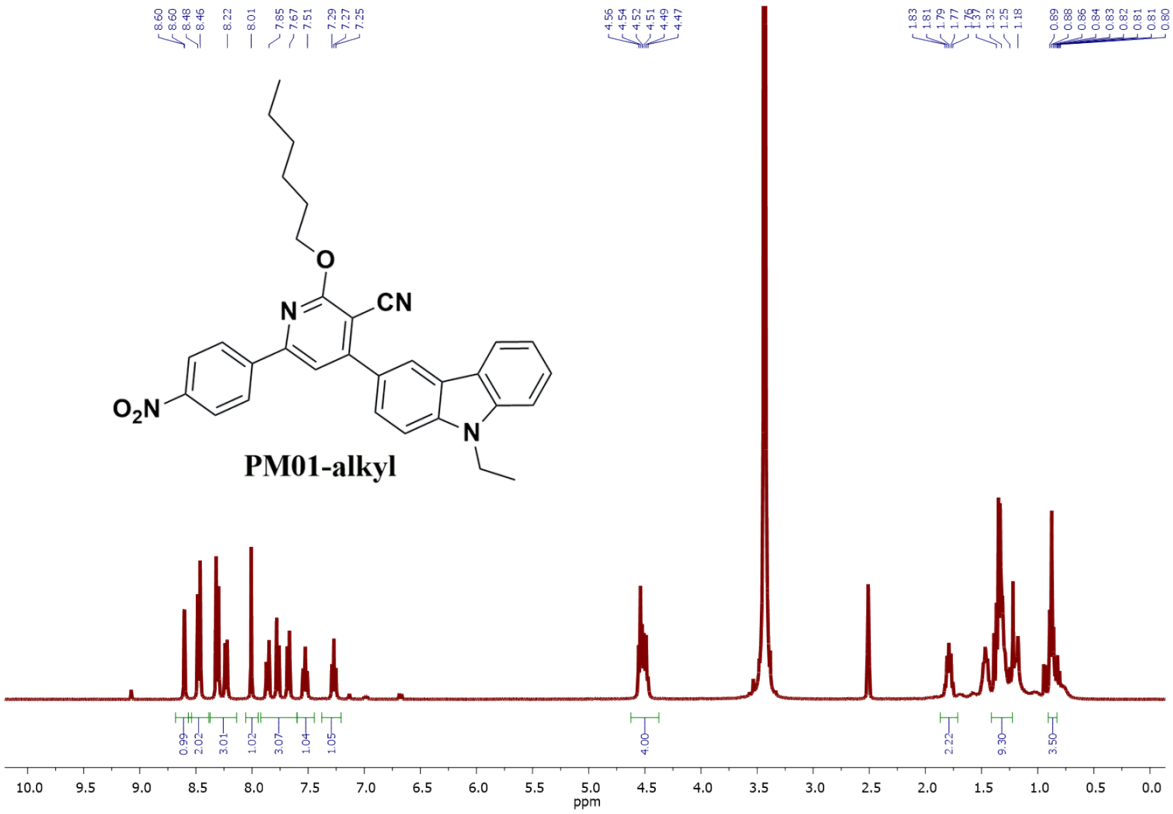

Fig. S9: ^{1}H NMR spectrum (400 MHz, DMSO-d_6) of **PM01-alkyl**.

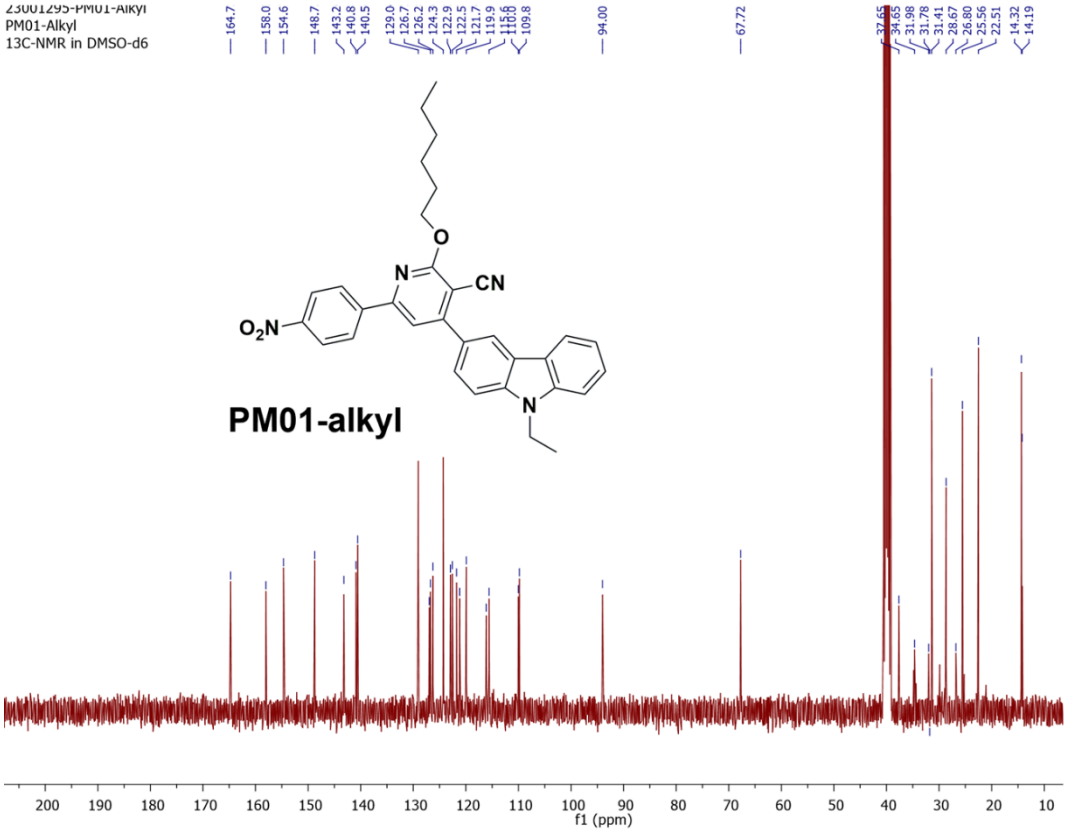

Fig. S10: ^{13}C NMR spectrum (100 MHz, DMSO-d_6) of **PM01-alkyl.**

6. Mass Spectra:

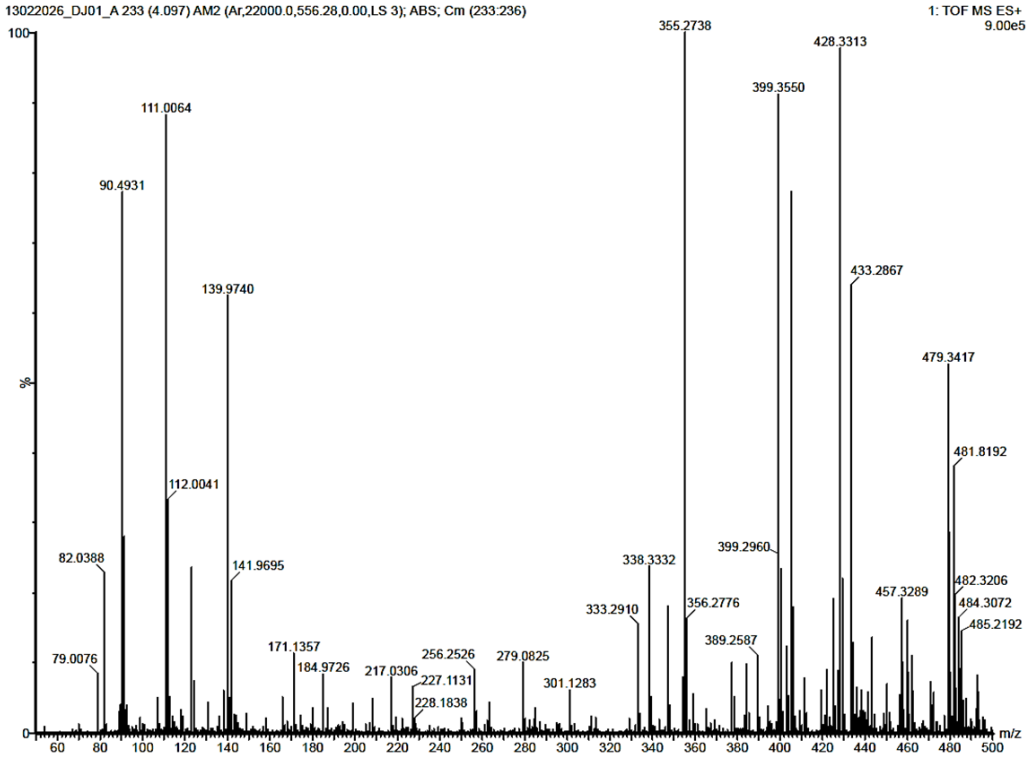

Fig. S11: HR-ESI-TOF MS of compound **DJ01-alkyl**.

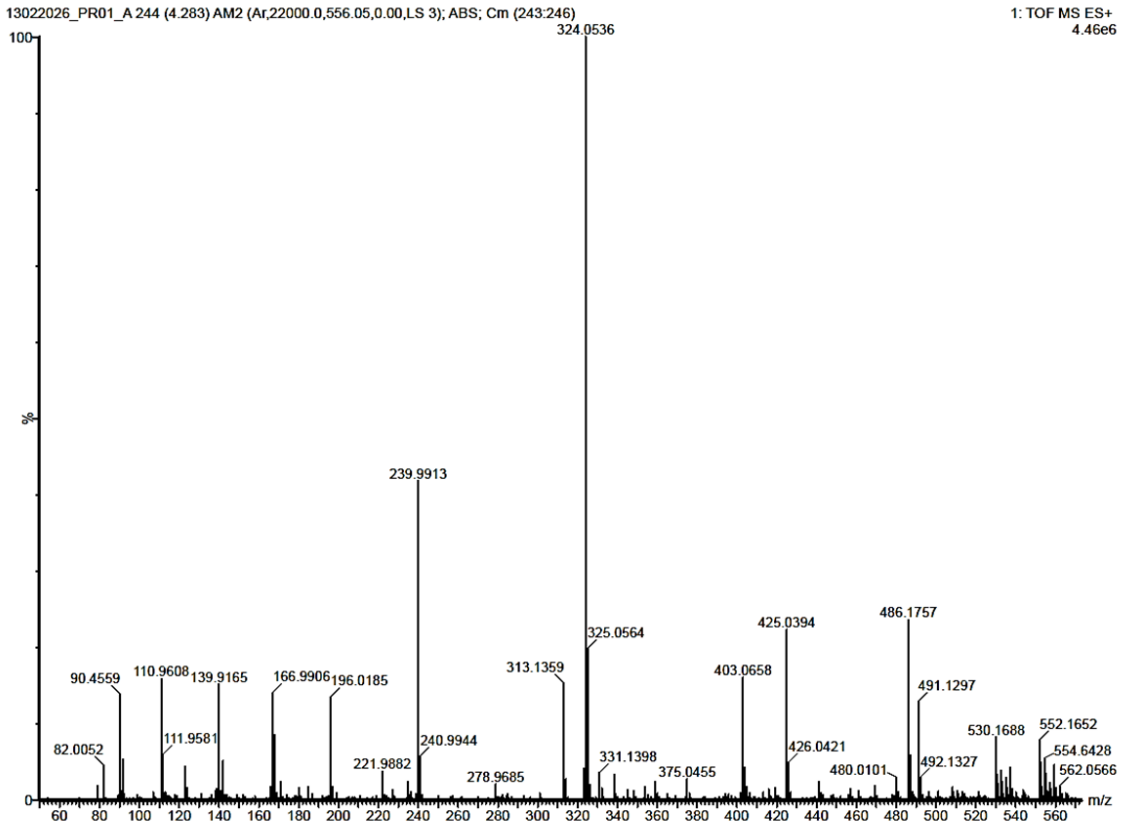

Fig. S12: HR-ESI-TOF MS of compound **PR01-alkyl**.

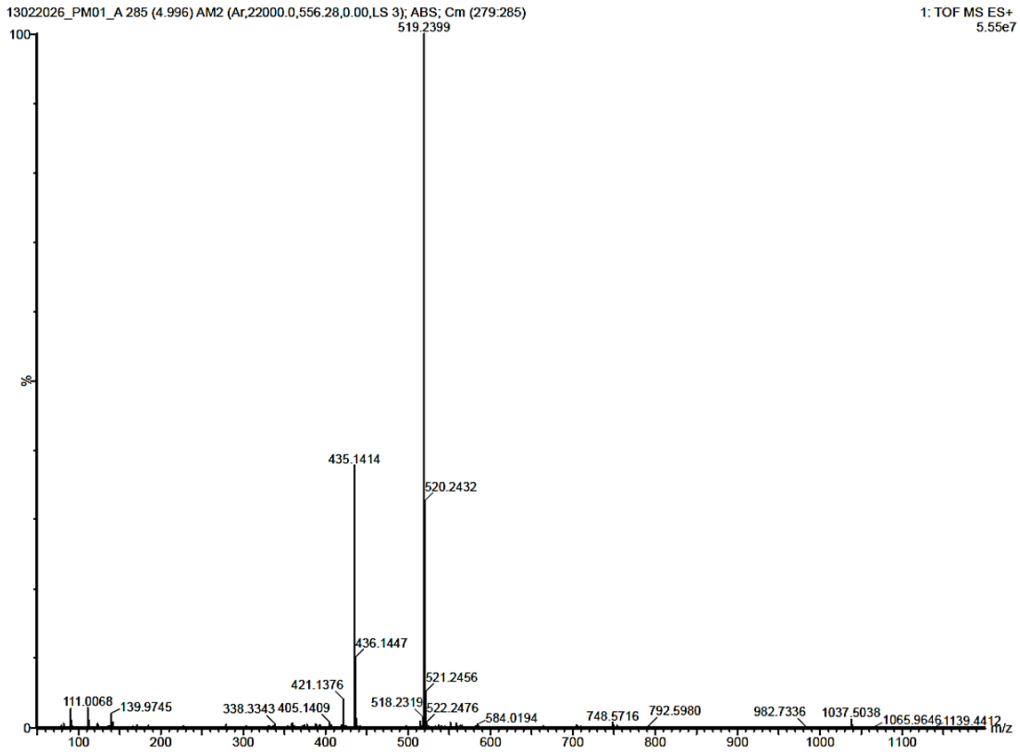

Fig. S13: HR-ESI-TOF MS of compound **PM01-alkyl**.

7. Photographic image

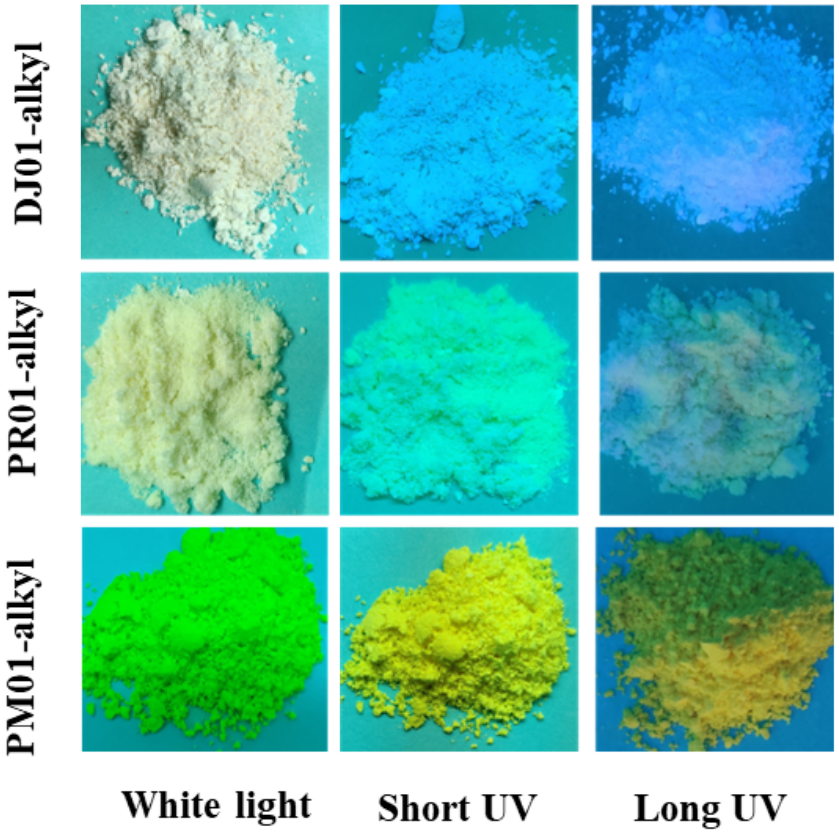

Fig. S14: Photographic images of **DJ01-alkyl; PR01-alkyl** and **PM01-alkyl** powders.

8. Contact Angle:

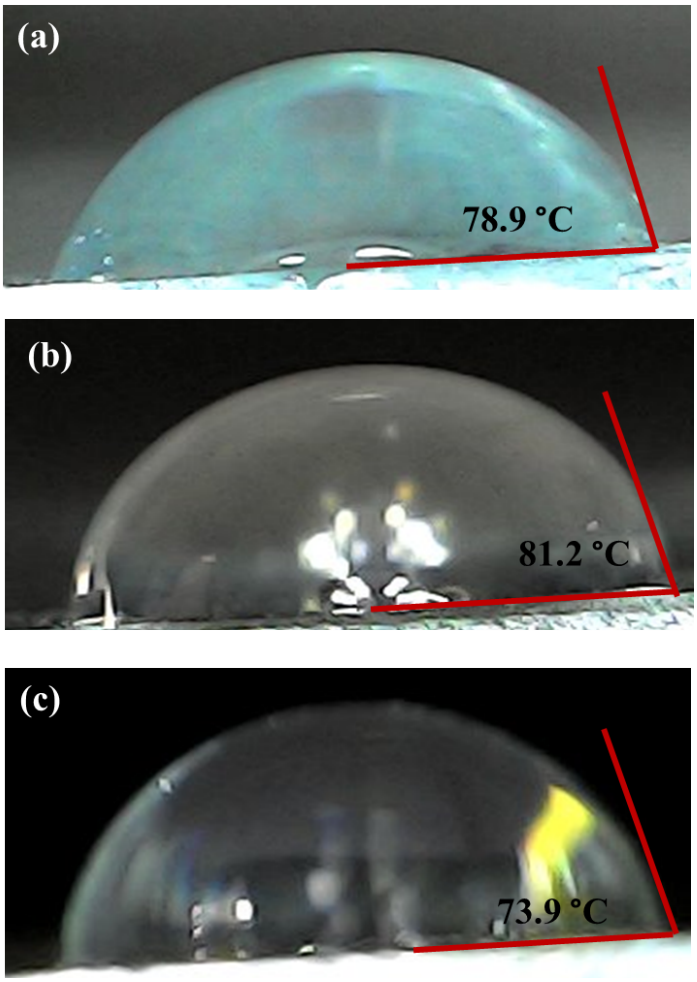

Fig. S15: Contact angle of (a) **DJ01-alkyl**; (b) **PR01-alkyl** and (c) **PM01-lkyl**.

9. Cyclic Voltammograms:

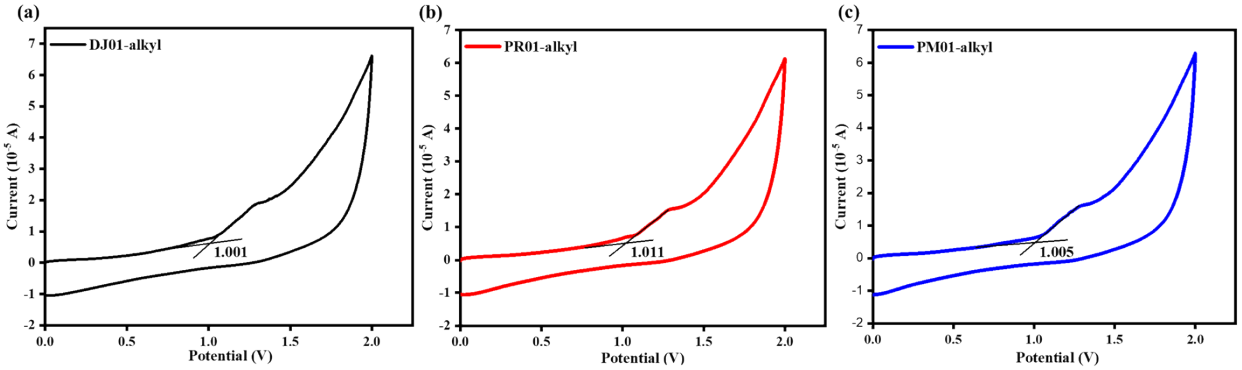

Fig. S16: Cyclic Voltammograms of (a) **DJ01-alkyl**; (b) **PR01-alkyl** and (c) **PM01-lkyl**.

9.1. Calculations:

DJ01-alkyl

$E_g(eV) = 1240/\lambda int$
λ_{int} = 418 nm
$E_g(eV) = 1240/418$
= 2.97 eV
$E_{HOMO} = -4.78+(E_{ox}(Fc)-E_{ox})$
$= -4.78 + (0.4076-1.001)$
= -5.37 eV
Where, E_{ox} (Fc) = 0.4076
$E_{LUMO} = E_g + E_{HOMO}$
= 2.97-5.37
= -2.40 eV

PR01-alkyl

$E_g(eV) = 1240/\lambda int$
λ_{int} = 424 nm
$E_g(eV) = 1240/424$
= 2.92 eV
$E_{HOMO} = -4.78+(E_{ox}(Fc)-E_{ox})$
$= -4.78 + (0.4076-1.011)$
= -5.38 eV
Where, E_{ox} (Fc) = 0.4076
$E_{LUMO} = E_g + E_{HOMO}$
= 2.97-5.38
= -2.46 eV

PM01-alkyl

$E_g(eV) = 1240/\lambda int$
λ_{int} = 415 nm
$E_g(eV) = 1240/415$
= 2.99 eV
$E_{HOMO} = -4.78+(E_{ox}(Fc)-E_{ox})$
$= -4.78 + (0.4076-1.005)$
= -5.37 eV
Where, E_{ox} (Fc) = 0.4076
$E_{LUMO} = E_g + E_{HOMO}$
= 2.97-5.37
= -2.38 eV

10. Output Files:

Table S7: Output file of DJ01-alkyl (B3LYP/6-311G(d).

C	-15.51018	-0.39508	1.40908
C	-14.45826	-0.70132	0.5922
C	-13.44911	0.25225	0.4445
C	-13.50195	1.42375	1.07274
C	-14.55861	1.77308	1.90972
C	-15.56438	0.85856	2.07394
C	-12.25025	2.18771	0.65532
C	-11.59616	1.353	-0.15005
C	-10.36671	1.71624	-0.69009
H	-9.83304	1.04059	-1.32996
C	-9.85001	2.95863	-0.37631
C	-10.56204	3.88353	0.45882
C	-11.77212	3.47803	0.99648
H	-16.3046	-1.09995	1.53863
H	-14.41942	-1.63874	0.07063
H	-14.59687	2.7294	2.3978
H	-16.39691	1.09019	2.70879
H	-8.89433	3.23107	-0.76455
H	-12.33316	4.12579	1.64597
C	-9.9529	5.33012	0.71049
C	-10.62	6.34384	1.34923
C	-8.67817	5.63717	0.29014

C	-10.08985	7.66903	1.35093
C	-8.28815	6.9498	0.24209
H	-8.00189	4.84511	-0.02674
N	-12.31613	0.18908	-0.30434
C	-11.93134	-0.97453	-1.15549
H	-12.33473	-0.84934	-2.14363
H	-10.86499	-1.03768	-1.21527
C	-12.48285	-2.28525	-0.54572
H	-12.07669	-2.42146	0.4349
H	-13.54847	-2.23283	-0.48808
H	-12.20054	-3.11603	-1.164
C	-11.94733	6.03701	2.0643
N	-12.94121	5.8072	2.59972
N	-9.03797	7.94663	0.67217
O	-10.77605	8.65884	2.16895
C	-9.952	9.54593	2.99625
H	-9.88743	10.5303	2.58992
H	-10.42586	9.57894	3.9595
C	-8.51025	9.00961	3.09731
H	-7.99497	9.38854	3.95026
H	-8.54676	7.94254	3.15766
C	-7.78042	9.53194	1.84227
H	-6.8206	9.08167	1.73047
H	-8.38425	9.30866	0.98885
C	-7.58569	11.09017	1.98883
H	-7.26767	11.49761	1.05564
H	-8.51793	11.52872	2.27997
C	-6.48241	11.43817	3.04001
H	-6.38649	12.50809	3.11874
H	-6.72895	11.03747	4.0016
C	-5.146	10.84387	2.54679
H	-4.93141	11.22982	1.56309
H	-4.35154	11.11845	3.22294
H	-5.22647	9.77188	2.50223

C	-6.90249	7.21683	-0.28792
C	-6.42131	8.33862	-0.97105
C	-4.48218	6.93974	-0.68094
H	-6.99757	9.19358	-1.2885
C	-4.89259	8.15301	-1.21642
H	-3.47446	6.6042	-0.6906
H	-4.26605	8.86381	-1.71385
S	-5.74015	6.15271	-0.09561

Table S8: Output file of PR01-alkyl (B3LYP/6-311G(d)

C	-1.10451	-4.08031	-0.97275
C	0.16787	-3.54617	-1.28738
C	0.88339	-2.87181	-0.23698
C	0.25683	-2.77952	0.96867
C	-0.98473	-3.28657	1.27508
C	-1.66884	-3.93691	0.33121
C	2.15798	-1.78301	1.34552
C	2.28443	-2.11276	0.0336
C	3.53358	-1.7212	-0.63506
H	3.70875	-1.95661	-1.66836
C	4.51373	-0.98056	0.17492
C	4.22646	-0.72465	1.51964
C	3.08512	-1.11541	2.07985
H	-1.67881	-4.59818	-1.7045
H	0.56589	-3.66329	-2.27492
H	-1.38236	-3.15711	2.26254
H	-2.62694	-4.34346	0.57206
H	4.93179	-0.19811	2.10977
H	2.88559	-0.9132	3.10741
C	5.93565	-0.38352	-0.22855
C	6.37817	-0.50435	-1.49931
C	6.83352	0.31686	0.67614
C	7.59614	0.04009	-1.87993
C	8.07145	0.80043	0.22539

H	6.5516	0.47639	1.69745
C	9.07515	1.56999	1.15567
C	8.729	1.81142	2.48262
C	10.29289	2.02471	0.69205
C	9.56881	2.4843	3.30576
H	7.79074	1.46365	2.85028
C	11.16351	2.72496	1.55359
H	10.58336	1.85156	-0.32203
C	10.80273	2.94785	2.83923
H	9.28496	2.66338	4.31772
H	12.1079	3.08393	1.19881
C	5.51902	-1.27672	-2.49531
N	4.87077	-1.8595	-3.24681
N	8.43113	0.62127	-1.03582
N	1.01228	-2.16172	1.81403
C	0.59538	-1.92312	3.17928
H	1.40255	-2.17311	3.83827
H	0.33504	-0.89984	3.30955
C	-0.63497	-2.78984	3.44812
H	-1.42678	-2.47816	2.79373
H	-0.40956	-3.816	3.27375
H	-0.94411	-2.65775	4.46356
O	7.89395	-0.06939	-3.23316
C	9.00972	0.5971	-3.78169
H	9.13216	0.19076	-4.74662
H	8.86432	1.67038	-3.85355
C	10.28166	0.32789	-2.94539
H	10.37101	1.04101	-2.13352
H	10.28802	-0.64682	-2.53281
C	11.36819	0.41787	-4.0105
H	11.276	1.35925	-4.49939
H	11.16676	-0.38801	-4.67202
C	12.82174	0.312	-3.59021
H	13.3958	0.26391	-4.4771

H	13.03512	-0.54949	-2.97554
C	13.17787	1.59238	-2.86646
H	12.68978	2.413	-3.33276
H	12.87039	1.53987	-1.83566
C	14.68346	1.80073	-3.02389
H	14.9764	2.69997	-2.54592
H	15.21836	0.97515	-2.60604
H	14.89548	1.85938	-4.07949
Br	11.97357	3.89278	4.01579

Table S9: Output file of PM01-alkyl (B3LYP/6-311G(d)

C	0.09692	-3.42061	-1.06152
C	1.3576	-2.86816	-1.23351
C	1.87558	-2.10904	-0.1678
C	1.1447	-1.89006	0.93457
C	-0.07619	-2.55312	1.18507
C	-0.60382	-3.30297	0.17297
C	3.06274	-0.88421	1.32892
C	3.235	-1.37155	0.10936
C	4.46763	-1.12572	-0.59103
H	4.63222	-1.48491	-1.58383
C	5.44652	-0.36988	0.11047
C	5.23729	-0.05312	1.47648
C	4.06785	-0.32852	2.08766
H	-0.36907	-3.94869	-1.86413
H	1.89789	-3.0152	-2.13824
H	-0.56633	-2.47908	2.12614
H	-1.54553	-3.80683	0.31668
H	6.02204	0.41471	2.04286
H	3.92025	-0.10915	3.11744
C	6.80528	0.18721	-0.45795
C	7.23539	0.03484	-1.75912
C	7.63682	0.90895	0.43466
C	8.50715	0.57055	-2.13414

C	8.86144	1.40618	0.01874
H	7.3217	1.06409	1.44596
C	9.80545	2.15307	1.03086
C	9.34866	2.45534	2.32897
C	11.11732	2.53278	0.66744
C	10.18858	3.11883	3.24633
H	8.36063	2.17967	2.61972
C	11.96451	3.17256	1.60004
H	11.48044	2.32987	-0.31994
C	11.49827	3.46637	2.88916
H	9.82645	3.35718	4.22421
H	12.96764	3.43473	1.32589
C	6.34874	-0.70639	-2.7769
N	5.68679	-1.25969	-3.53648
N	9.2452	1.23563	-1.25445
O	9.06714	0.3966	-3.45716
C	10.48534	0.40536	-3.22451
H	10.64648	-0.10662	-2.30018
H	11.0029	-0.09765	-4.01446
C	11.04838	1.85317	-3.12772
H	12.03344	1.81406	-2.71699
H	10.41327	2.43587	-2.49228
C	11.1763	2.49857	-4.53742
H	11.84286	1.89476	-5.11876
H	10.2271	2.55288	-5.02964
C	11.77376	3.92286	-4.38566
H	12.65547	3.87305	-3.7835
H	11.0507	4.55653	-3.91496
C	12.17132	4.49983	-5.76516
H	12.91886	3.86898	-6.20436
H	11.31921	4.54172	-6.40771
C	12.74669	5.92212	-5.57852
H	13.58604	5.88498	-4.91403
H	13.06122	6.30939	-6.52602

H	11.99338	6.55913	-5.16545
N	12.37259	4.13678	3.874
O	13.66191	4.43753	3.55903
O	11.94706	4.41625	4.95866
N	1.79557	-0.98018	1.69349
C	1.31025	-0.11139	2.75734
H	1.98966	-0.1644	3.58298
H	1.26038	0.89217	2.38974
C	-0.0985	-0.4783	3.1919
H	-0.74553	-0.47953	2.34004
H	-0.10846	-1.44221	3.64694
H	-0.43869	0.25301	3.89828

References:

1. Sheldrick, G. M., SHELXT–Integrated space-group and crystal-structure determination. *J Foundations of Crystallography* **2015,** *71* (1), 3-8.

2. Sheldrick, G. M. J. C. S. C., Crystal structure refinement with SHELXL. *Crystal Structure Communications* **2015,** *71* (1), 3-8.

3. Dolomanov, O. V.; Bourhis, L. J.; Gildea, R. J.; Howard, J. A.; Puschmann, H. J. A. C., OLEX2: a complete structure solution, refinement and analysis program. *Applied Crystallography* **2009,** *42* (2), 339-341.

4. Yu, W.; Yang, Q.; Zhang, J.; Tu, D.; Wang, X.; Liu, X.; Li, G.; Guo, X.; Li, C., Simple Is Best: A p-Phenylene Bridging Methoxydiphenylamine-Substituted Carbazole Hole Transporter for High-Performance Perovskite Solar Cells. *ACS Applied Materials & Interfaces* **2019,** *11* (33), 30065-30071.

5. Liu, X.; Ma, S.; Ding, Y.; Gao, J.; Liu, X.; Yao, J.; Dai, S., Molecular Engineering of Simple Carbazole-Triphenylamine Hole Transporting Materials by Replacing Benzene with Pyridine Unit for Perovskite Solar Cells. *Solar RRL* **2019,** *3* (5), 1800337.

6. Yin, X.; Guan, L.; Yu, J.; Zhao, D.; Wang, C.; Shrestha, N.; Han, Y.; An, Q.; Zhou, J.; Zhou, B.; Yu, Y.; Grice, C. R.; Awni, R. A.; Zhang, F.; Wang, J.; Ellingson, R. J.; Yan, Y.; Tang, W., One-step facile synthesis of a simple carbazole-cored hole transport material for high-performance perovskite solar cells. *Nano Energy* **2017,** *40*, 163-169.

7. Zhai, M.; Miao, Y.; Chen, C.; Liu, L.; Wang, H.; Ding, X.; Xia, Z.; Wang, L.; Cheng, M., Modulating donor assemblies of D-π-D type hole transport materials for perovskite solar cells. *Journal of Power Sources* **2022,** *551*, 232199.

8. Qin, T.; Wu, F.; Mu, Y.; Long, Y.; Zhu, L.; Zhao, J.; Chi, Z., Sulfonyldibenzene-based hole-transporting materials for efficient n-i-p perovskite solar cells. *Science China Chemistry* **2021,** *64* (1), 127-133.

9. Liu, X.; Ding, X.; Ren, Y.; Yang, Y.; Ding, Y.; Liu, X.; Alsaedi, A.; Hayat, T.; Yao, J.; Dai, S., A star-shaped carbazole-based hole-transporting material with triphenylamine side arms for perovskite solar cells. *Journal of Materials Chemistry C* **2018,** *6* (47), 12912-12918.

10. Liu, X.; Shi, X.; Liu, C.; Ren, Y.; Wu, Y.; Yang, W.; Alsaedi, A.; Hayat, T.; Kong, F.; Liu, X.; Ding, Y.; Yao, J.; Dai, S., A Simple Carbazole-Triphenylamine Hole Transport Material for Perovskite Solar Cells. *The Journal of Physical Chemistry C* **2018,** *122* (46), 26337-26343.

11. Li, M.; Ma, S.; Mateen, M.; Liu, X.; Ding, Y.; Gao, J.; Yang, Y.; Zhang, X.; Wu, Y.; Dai, S., Facile donor (D)-π-D triphenylamine-based hole transporting materials with different π-linker for perovskite solar cells. *Solar Energy* **2020,** *195*, 618-625.

12. Sutanto, A. A.; Joseph, V.; Igci, C.; Syzgantseva, O. A.; Syzgantseva, M. A.; Jankauskas, V.; Rakstys, K.; Queloz, V. I. E.; Huang, P.-Y.; Ni, J.-S.; Kinge, S.; Asiri, A. M.; Chen, M.-C.; Nazeeruddin, M. K., Isomeric Carbazole-Based Hole-Transporting Materials: Role of the Linkage Position on the Photovoltaic Performance of Perovskite Solar Cells. *Chemistry of Materials* **2021,** *33* (9), 3286-3296.

13. Chetri, R.; T.N, A., Minireview and Outlook of Carbazole and Phenothiazine-Modified Triphenylamines as Hole Transporting Materials for Enhancing Perovskite Solar Cells. *Energy & Fuels* **2025,** *39* (20), 9232-9261.

14. Chetri, R.; Devadiga, D.; Rakstys, K.; Jankauskas, V.; Getautis, V.; Ghadari, R.; Nazeeruddin, M. K.; Tantri Nagaraja, A., D–A–D- and A–A–D-Type Cyanopyridone Derivatives as a New Class of Hole-Transporting Materials for Perovskite Solar Cells. *Energy & Fuels* **2024**.